A NUMERICAL CALCULATION OF THE PENETRATION FACTOR AND ITS APPLICATION

Vinh N.T. Pham[a], N.N. Duy[b,c,†], K.Y. Chae[c]
N. Nhu Le[d], T.V. Nhan Hao[d]

[a]Department of Physics, Ho Chi Minh City University of Education
Ho Chi Minh City 748342, Vietnam
[b]Institute of Research and Development, Duy Tan University
Da Nang 550000, Vietnam
[c]Department of Physics, Sungkyunkwan University
Suwon 16419, South Korea
[d]Faculty of Physics, University of Education, Hue University
34 Le Loi Street, Hue City 530000, Vietnam

(Received December 11, 2019; accepted March 5, 2020)

In this study, we develop a computer code called Numerical Calculation of the Penetration Factor (NCPF) for calculation of the penetration factor in nuclear interactions. The code is valid in both low-energy thermonuclear reactions for astrophysical applications and high-energy interactions of heavy nuclei. Our validation results indicate that this code can be successfully used to determine the penetrability for calculations of the partial widths of thermonuclear reactions and the half-lives of heavy isotopes. By using the code, we evaluate the astrophysical rates of the $^{22}\mathrm{Mg}(\alpha,p)^{25}\mathrm{Al}$ reaction and the α-decay half-lives of super-heavy nuclei with atomic numbers up to $Z = 118$.

DOI:10.5506/APhysPolB.51.973

1. Introduction

Quantum tunneling [1–3] of particles through a nuclear interaction barrier is one of the fundamental concepts for understanding the transmission phenomena of nuclear systems. The barrier penetrability (or penetration factor) of a charged particle is important for estimation of the cross sections of thermonuclear reactions and the α-decay half-lives of heavy nuclei. In studies of the nucleosynthesis of stars, the cross sections of the thermonuclear reactions are often calculated by using the Breit–Wigner formula

† Corresponding author: nguyenngocduy9@duytan.edu.vn

regarding the resonance strength [4] of these reactions due to the challenge of the small yields and limitations of the radioactive beam intensity in direct measurements. In the synthesis of super-heavy nuclides, the feasibility of observing new elements can be evaluated through the α-decay half-lives which are closely associated with the penetration factor [5, 6]. Therefore, quantification of the penetrability is vital to nuclear research.

It is difficult to calculate the penetration factor due to the complication of the Coulomb functions. Hence, only a few approaches to solving this obstacle have been reported such as approximation of either the interacting potential or the Coulomb functions. In cases of high-energy interactions, the penetrability is calculated based on the approximation of the potential barrier [5–11]. For instance, in the study by Li *et al.* [6], the penetration factor was calculated based on the parabolic potential barrier, which was described by the Wentzel–Kramers–Brillouin (WKB) approximation [5, 7, 10, 11]. The potential was divided into two parts at the barrier position, and then the penetrability was described as an exponential function of two terms related to the two parts of the potential. However, this approximation is only applicable in high-energy cases such as the α-decay or fusion reactions of heavy nuclei. The parabolic approximation of the potential [5, 10] is not appropriate to energies much smaller than the nuclear barrier that are associated with low-energy thermonuclear reactions in nucleosynthesis. An alternative way to approximate the penetration factor, which was based on the approximation of Coulomb functions proposed by Abramowitz and Stegun [12], was applied to the study of the $^{9}\mathrm{Be}(p,\alpha)^{6}\mathrm{Li}$ reaction cross section in Ref. [13]. This approach is solely reliable in the low-energy regime, which is appropriate for sub-threshold and near the threshold of the thermonuclear reactions. In general, these existing approximation approaches are mostly appropriate for specific cases to deal with different aspects of the limitations of the Coulomb functions.

Although the calculation of the penetrability is important in nuclear physics, computer codes for calculating this factor are still very limited. There are a few codes reported in the literature, but they either are not published or have limited applicability. For instance, there is a code called PENE programmed by Wiescher [14] at the University of Notre Dame for computing the penetrability, but it is not widely contributed for being used. Another code for calculating penetrability, ckin, was designed by Wheldon [15, 16] at the University of Birmingham based on the CERN Libraries WCLBES code [17]. Both of these codes are applicable to the low-energy reactions, and their algorithms are not described in detail. Hence, the development of a computer code for the calculation of the penetration factor in terms of the Coulomb functions for arbitrary energy is still highly demanded.

In the present work, we introduce a computer code named NCPF (Numerical Calculation of Penetration Factor) for the numerical calculation of the penetration factor in a wide range of energy cases from below the threshold of thermonuclear reactions to arbitrarily high energy. The code is developed mainly based on the Steed method [18, 19] for evaluation of the Coulomb functions. There exists a turning point associated with a critical interacting energy $E_{\rm cr}$ due to the interaction between two positively-charged particles, because of which Steed's method collapses in the range of $E < E_{\rm cr}$ corresponding to the low-energy regime. In this regime, the approximation proposed by Abramowitz and Stegun [12] is used. In order to validate the reliability and applicability of the code, it is then applied to evaluate the penetration factor for determining the partial widths of astrophysical reactions ($^{12}{\rm C}(\alpha,\gamma)^{16}{\rm O}$ and $^{26}{\rm Si}(\alpha,p)^{29}{\rm P}$) and the α-decay half-lives of heavy nuclei with $Z = 52$–118 corresponding to the low- and high-energy ranges, respectively. The results show that the calculation using this current code is in good agreement with previous works. Once the code successfully reproduced the values of the previous studies, we then applied it to deduce the penetration factor for the new results in the calculations of the astrophysical rates of the $^{22}{\rm Mg}(\alpha,p)^{25}{\rm Al}$ reaction which has not been reported in the literature so far.

The present paper is organized as follows. The theoretical framework for the numerical calculations and the algorithms of the code are presented in Section 2. The validation and applications of the code are described in Section 3. The validation of the code for the thermonuclear reactions is detailed in Section 3.1. The new results of the astrophysical rates of the important stellar reaction $^{22}{\rm Mg}(\alpha,p)^{25}{\rm Al}$ in the rp-process are analyzed and discussed in Section 3.2. The evaluation of the α-decay half-life of the superheavy nuclei up to $Z = 118$ is presented in Section 3.3. The paper is summarized in the final section, Section 4.

2. Theoretical framework

The penetration factor of a projectile in a nuclear reaction can be read in terms of radial Coulomb wave functions as

$$P_l(\eta,\rho) = \frac{1}{F_l^2(\eta,\rho) + G_l^2(\eta,\rho)}\,, \tag{1}$$

where $F_l(\eta,\rho)$ and $G_l(\eta,\rho)$ are the regular and irregular Coulomb functions [12], respectively, and l is the angular momentum of the projectile. The functions in Eq. (1) are conventionally characterized by the Sommerfeld parameter η, and the dimensionless variable ρ, which is associated with the centrifugal barrier. Notice that, in principle, the Sommerfeld parameter

can be negative for atomic scattering as well as positive in the case of nuclear interactions. These parameters can be read as [4]

$$\eta = \frac{e^2}{4\pi\varepsilon_0\hbar} Z_1 Z_2 \left(\frac{\mu}{2E}\right)^{1/2}, \tag{2}$$

$$\rho = \left(\frac{2\mu E R^2}{\hbar}\right)^{1/2}, \tag{3}$$

where Z_1, Z_2, μ, and E are the atomic numbers, reduced mass, and energy in the center-of-mass frame of the charged particles, respectively. Here, $R = R_0(A_1^{1/3} + A_2^{1/3})$ is the effective distance between two nuclei and $R_0 = 1.25$ fm. A_1 and A_2 denote the mass numbers of the projectile and target of the nuclear interacting system.

The calculation of the penetration factor requires high accuracy of the Coulomb functions. These functions are usually associated with the Coulomb scattering problem, earning that the particles have positive relative energy. In 1964, Curtis [20] first proposed a method for considering this problem for $\eta < 0$ restricted to $l = 0, 1, 2$, which was numerically certified by Barnett in 1974 [21]. The general cases for all real η and ρ were comprehensively considered by Bardin *et al.* in 1972 [22]. An extension for electron scattering dealing with negative energies was proposed by Bell and Scott in 1980 [23]. Meanwhile, in 1982, the more general treatment for all cases of energies was proposed by Seaton [24]. Despite the fact that these approaches are more or less successful in giving the results of Coulomb functions, they are all based on some approximation such as series expansion in powers of ρ or ρ^{-1} asymptotically. Another approach treating negative energy was introduced in 2010 by Peng and Gong [25] for considering the hydrogenic continuum wave functions in a wide range of energy and radial distance without any restriction to the angular momentum number. However, this work deals only with the regular solution $F_l(\eta, \rho)$ for $\eta < 0$ [25].

In this paper, we adopted the approach proposed by Steed in 1967 [19], in which two Coulomb functions and their derivatives are calculated in an interdependent manner. This approach is based on two continued fractions in terms of the Coulomb functions. For the regular function and its first derivative, the fraction reads

$$\frac{F_l'(\eta,\rho)}{F_l(\eta,\rho)} = \frac{l+1}{\rho} + \frac{\eta}{l+1} - \rho\left((l+1)^2+\eta^2\right)\frac{(l+2)}{(l+1)}\frac{H_{l+2}H_{l+3}}{K_{l+1}+K_{l+2}+K_{l+3}+\ldots}, \tag{4}$$

where the functions of $H_m(\eta, \rho)$ and $K_n(\eta, \rho)$ can be taken from

$$H_m = -\rho^2\left(m^2+\eta^2\right)\left(m^2-1\right); \qquad m = l+2, l+3, \ldots \tag{5}$$

$$K_n = (2n+1)\left[\eta\rho + n(n+1)\right]; \qquad n = l+1, l+2, \ldots \tag{6}$$

The second fraction for the complex functions in terms of two regular Coulomb functions and their first derivatives is then given as

$$\frac{G_l'(\eta,\rho) \pm iF_l'(\eta,\rho)}{G_l(\eta,\rho) \pm iF_l(\eta,\rho)} = \frac{1}{\rho}\left((\rho-\eta)i + \frac{i(i\eta-l)(i\eta+l+1)(i\eta-l+1)(i\eta+l+2)}{2(\rho-\eta+i)+2(\rho-\eta+2i)+\ldots}\right). \quad (7)$$

The original version of the program based on the method of Steed, RCWFN, was first published by Barnett *et al.* in 1974 [21]. The improved and comprehensive version, COULFG, was introduced by Barnett in 1982 [26]. In that paper, they provided a comprehensive description of the algorithm and results from comparison of their codes, which used two different methods, RCWFN and COULFG. To develop our NCPF code in Fortran 90 for the purpose of calculating the penetration factor, we mainly employed the newest version of this program, COUL90, which was introduced in 1996 by Barnett [18]. Note that the vital difference of COUL90 from its predecessor is the utilization of the LT algorithm [27] for forward evaluating of the first continued fraction (refer to Ref. [18] for detailed description).

Since we are dealing with the interaction between two positively charged particles, there exists a turning point $\rho_{\rm cr}$ of the second-order differential equation governing the Coulomb functions. This parameter is determined as [18]

$$\rho_{\rm cr} = \eta + \left[\eta^2 + l(l+1)\right]^{1/2}. \quad (8)$$

The version COUL90 is appropriate in providing highly accurate Coulomb functions $F_l(\eta,\rho)$ and $G_l(\rho,\rho_{\rm cr})$ provided $\rho > \rho_{\rm cr}$, corresponding to the high-energy range of $E > E_{\rm cr}$. This turning point is associated with the critical relative energy $E_{\rm cr}$ considered as the minimum value for COUL90 to work properly, and straightforwardly determined by substituting Eqs. (2) and (3) into Eq. (8) as

$$E_{\rm cr} = \frac{\hbar^2}{2}\frac{l(l+1)}{\mu R^2} + \alpha\hbar c\frac{Z_1 Z_2}{R}, \quad (9)$$

where α and c are the fine-structure constant and speed of light in vacuum, respectively. For the low-energy regime $E < E_{\rm cr}$ corresponding to $\rho < \rho_{\rm cr}$, an alternative approach has been considered. We used the asymptotic behavior of the functions, which are explicitly given in analytical form as presented by Abramowitz and Stegun (AS approximation) [12]

$$F_l(\eta,\rho) \approx \frac{(2l+1)!C_l(\eta)}{(2\eta)^{l+1}}(2\eta\rho)^{1/2} I_{2l+1}\left[2(2\eta\rho)^{1/2}\right], \quad (10)$$

$$G_l(\eta,\rho) \approx \frac{2(2\eta)^{l}}{(2l+1)!C_l(\eta)}(2\eta\rho)^{1/2} K_{2l+1}\left[2(2\eta\rho)^{1/2}\right], \quad (11)$$

in which I_{2l+1} and K_{2l+1} are modified Bessel functions of the first and second kinds [12], which can be straightforwardly calculated using the integration method proposed by Schwartz in 2012 [27]. The factor $C(\eta)$ is described in terms of the Gamma function as [12]

$$C(\eta) = 2^l \exp\left(-\frac{\pi\eta}{2}\right) \frac{|\Gamma(l+1+i\eta)|}{\Gamma(2l+2)}\,. \tag{12}$$

Note that the Gamma function in Eq. (12) has a complex argument and it can be simply calculated by Lanczos approximation [28]. We also note that the use of this approximation for $F_l(\eta,\rho)$ and $G_l(\eta,\rho)$ in calculating the penetration factor for nuclear reactions of astrophysical interest in the low-energy regime was investigated in the work of Humblet *et al.* in 1987 [9]. This work also indicated the applicability of the approximation.

The main structure of the NCPF program is in a simple way illustrated in Fig. 1. Firstly, the program reads the input data including the Z and A of two nuclei, and the desired range of angular momentum [$l_{\min}$–$l_{\max}$] is also

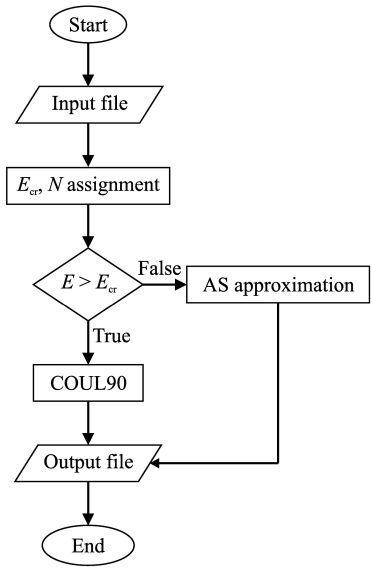

Fig. 1. Diagram of the algorithm used in the NCPF computer code.

included. In calculations for a specific l, one simply sets $l_{\min} = l_{\max}$. The program automatically determines the value of $E_{\rm cr}$ in Eq. (9) for each l; the normalization factor of AS approximation is also calculated as

$$N = \frac{P_l(\eta,\rho)_{|E=E_{\rm cr}^+}}{P_l(\eta,\rho)_{|E=E_{\rm cr}^-}}\,, \tag{13}$$

where $P_l(\eta,\rho)|_{E=E_{\rm cr}^+}$ and $P_l(\eta,\rho)|_{E=E_{\rm cr}^-}$ are calculated by Steed's method for the case where energy E is infinitesimally higher than $E_{\rm cr}$, and by the AS approximation at $E_{\rm cr}$, respectively. Note that this normalization factor N has been taken into account only for the AS approximation to guarantee the continuity of penetration factor as a function of energy E for any value of l.

Subsequently, the interacting energy in the center-of-mass frame E is considered. In the situation where $E > E_{\rm cr}$, the program uses Steed's method for calculation of the penetration factor, whereas for $E \leq E_{\rm cr}$, the AS approximation is adopted including the normalization factor N in Eq. (13).

3. Results and discussion

3.1. NCPF for thermonuclear reactions

Since nuclear processes always occur in the universe, nuclear reactions are thought to be the keys to solve astrophysical problems. For instance, the $^{12}\mathrm{C} + \alpha$ reaction is deserved to revisit since the $^{4}\mathrm{He}(\alpha\alpha,\gamma)^{12}\mathrm{C}$ and $^{12}\mathrm{C}(\alpha,\gamma)^{16}\mathrm{O}$ reactions are the main processes in helium burning. The $^{12}\mathrm{C}(\alpha,\gamma)^{16}\mathrm{O}$ reaction rates have a strong influence on the associated nucleosynthesis in the evolution of low-mass stars to massive ones. On the other hand, the $^{26}\mathrm{Si}(\alpha,p)^{29}\mathrm{P}$ reaction rates play a crucial role in revealing the anomalies in astrophysical observations related to the peak separation of 4–7 s in the bolometric luminosity of X-ray bursts of 4U/MXB 1636-53, 4U 1608-52 and GX 17+2; and the ratios of $^{26}\mathrm{Al}/^{27}\mathrm{Al}$ and $^{60}\mathrm{Fe}/^{26}\mathrm{Al}$ [29–31]. Unfortunately, there have been no direct measurements of these reactions so far, and their astrophysical rates are very uncertain and require more accurate studies.

The rates are often theoretically calculated based on the α-width value; however, due to the lack of experimental constrains on this quantity to date [32, 33], the width is frequently determined based on the penetration factor (P_l) as [4]

$$\Gamma_l = \frac{3\hbar^2}{\mu R^2} P_l(E,R) C^2 S\,, \tag{14}$$

where $\hbar = 1.054 \times 10^{-34}$ J s; μ, C, and S are the reduced mass, the Clebsch–Gordan coefficient and the spectroscopic factor, respectively.

To confirm the validity and applicability of NCPF, the computer code is first applied to evaluate the nuclear interacting barrier penetrability of the $^{12}\mathrm{C} + \alpha$ and $^{26}\mathrm{Si} + \alpha$ reactions. The center-of-mass energies are in the range of $E = 0.01$–3.0 MeV, which correspond to the stellar temperatures of $T_9 = 0.01$–3.5 GK (GigaKelvin) for the $^{12}\mathrm{C}(\alpha,\gamma)^{16}\mathrm{O}$ and $T_9 = 0.01$–3.0 GK for the $^{26}\mathrm{Si}(\alpha,\mathrm{p})^{29}\mathrm{P}$ reactions. Table I presents the comparison of the results calculated by the original COUL90 code and by NCPF in this work for the

$^{12}\mathrm{C} + \alpha$ system in the low-energy range of $E = 0.1$–1.0 MeV. In particular, the improvement of the NCPF code using the AS approximation overcomes the inapplicability of the COUL90 code for the energies $E < 0.3$ MeV, as can be seen in the left panel of Fig. 2.

TABLE I

The penetration factors with $l = 2$ for the $^{12}\mathrm{C}+\alpha$ system calculated by the COUL90 and NCPF codes. NCPF overcomes the inapplicability of COUL90 in the low-energy region of $E < 0.3$ MeV.

E [MeV]	$P_l^{\text{This work}}$	P_l^{COUL90}	E [MeV]	$P_l^{\text{This work}}$	P_l^{COUL90}
0.05	1.41×10^{-25}	2.04×10^{-22}	0.30	7.23×10^{-12}	7.23×10^{-12}
0.10	9.75×10^{-24}	1.29×10^{-20}	0.45	5.55×10^{-09}	5.55×10^{-09}
0.15	1.12×10^{-18}	1.11×10^{-15}	0.60	2.88×10^{-07}	2.88×10^{-07}
0.20	1.59×10^{-15}	1.24×10^{-12}	0.80	8.40×10^{-06}	8.40×10^{-06}
0.25	2.03×10^{-13}	1.30×10^{-10}	1.00	8.02×10^{-05}	8.02×10^{-05}

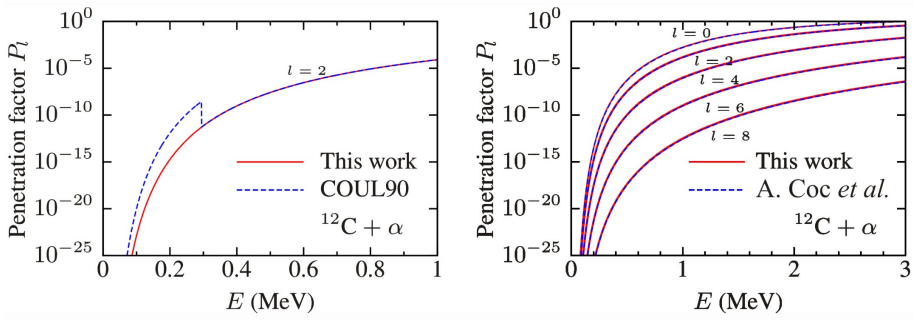

Fig. 2. Penetration factors of the $^{12}\mathrm{C} + \alpha$ system calculated by NCPF and COUL90 codes. Left panel: the inapplicability of the COUL90 in the low-energy region $E < 0.3$ MeV. Right panel: the NCPF results (solid curves) are consistent with those evaluated by Coc *et al.* [32] (dashed curves).

The penetration factor of the $^{12}\mathrm{C} + \alpha$ channel is computed with all possible angular momenta of $l = 0$–8 in the mentioned astrophysical energy region by using the NCPF code. The right panel of Fig. 2 shows the penetration factors as a function of energy for five representative values of angular momentum. As shown, the NCPF code effectively reproduces the penetrability obtained by Coc *et al.* [32]. Notice that the penetration factor defined by Coc *et al.* differs from Eq. (1) by a factor ρ. It also indicates that the Coulomb barrier penetration is mostly populated with the s-wave resonance ($l = 0$) of the alpha particle. The nuclear barrier penetration factor increases with the energy of the reaction as expected and decreases as l grows due to the emergence of centrifugal potential.

We continue to reproduce the α-width of the ^{26}Si$(\alpha, p)^{29}$P reaction by using the resonance parameters obtained by Almaraz-Calderon *et al.* [34] to doubly validate the NCPF code for the low-energy range. The angular momenta are deduced based on the spin-parity values of the resonant states of the compound nucleus, ^{30}S [34], as shown in Table II. The α-widths calculated using Eq. (14), in which the penetration factor is determined by employing our NCPF code, are presented in Fig. 3. The results are again consistent with those obtained by Almaraz-Calderon *et al.* [34]. This consistency reflects the capability of NCPF in the penetrability calculation for the low-energy thermonuclear reactions to which COUL90 could not be applied.

TABLE II

Resonance parameters were used to deduce the α-partial width of the ^{30}S nucleus [34].

E [MeV]	J^π	l	C^2S	E [MeV]	J^π	l	C^2S
0.0484	2+	2	0.01	1.6724	4+	4	0.01
0.1430	1−	1	0.01	1.7570	3−	3	0.01
0.3582	2+	2	0.01	1.8570	3−	3	0.01
0.4421	0+	0	0.01	1.9570	4+	4	0.01
0.5312	2+	2	0.01	2.0567	4+	4	0.01
0.6658	4+	4	0.01	2.1474	4+	4	0.01
0.7275	0+	0	0.01	2.2032	1−	1	0.01
0.7796	4+	4	0.01	2.2661	4+	4	0.01
0.9317	2+	2	0.01	2.3387	3−	3	0.01
1.1001	3−	3	0.01	2.4270	4+	4	0.01
1.3070	3−	3	0.01	2.5093	3−	3	0.01
1.4121	3−	3	0.01	2.6962	0+	0	0.01
1.4719	4+	4	0.01				

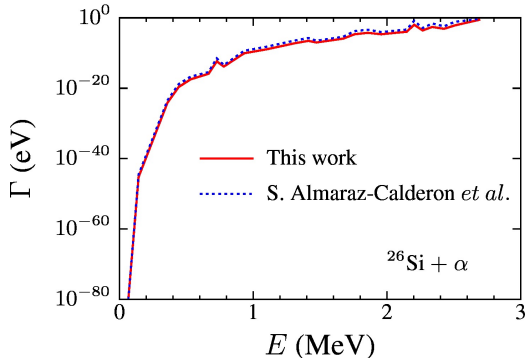

Fig. 3. (Color online) The α-partial widths of the ^{26}Si + α scattering reproduced by using the penetration factor computed by NCPF code (solid red curve) are in good agreement with the results obtained by Almaraz-Calderon *et al.* [34] (dotted curve).

3.2. Evaluation of the $^{22}Mg(\alpha,p)^{25}Al$ reaction rates

The astrophysical rates of the ^{22}Mg$(\alpha,p)^{25}$Al reaction under stellar conditions of $T_9 = 0.01$–3.0 GigaKelvin (GK) corresponding to the Gamow energy range of $E = 0.05$–4.25 MeV, also play a key role in understanding anomalies in astrophysical observations such as the Ne-E problem, the 1.275-MeV gamma ray and the abundance of ^{22}Na [35–38]. This gamma ray is predicted to be emitted from the excited ^{22}Ne* nuclide that is produced by the beta decay of ^{22}Na$(\beta^+)^{22}$Ne* in the rp-process, as can be seen in Fig. 4. The production mechanism of the gamma ray with the energy of 1.275-MeV is similar to that of the 1.809-MeV gamma ray that is emitted from the excited state of ^{26}Mg. However, although the 1.809-MeV gamma line was observed in 1983, the 1.275-MeV one has not been detected to date. This phenomenon is thought to be caused by the dominance of the ^{22}Mg$(\alpha,p)^{25}$Al and/or the ^{22}Mg$(p,\gamma)^{23}$Al reaction, which may skip the beta decays of ^{22}Mg$(\beta^+)^{22}$Na$(\beta^+)^{22}$Ne, resulting in the variations of the ^{20}Ne/^{22}Ne and the ^{22}Na abundance [35–38]. Therefore, studies of the astrophysical rates of the concerned reactions are needed.

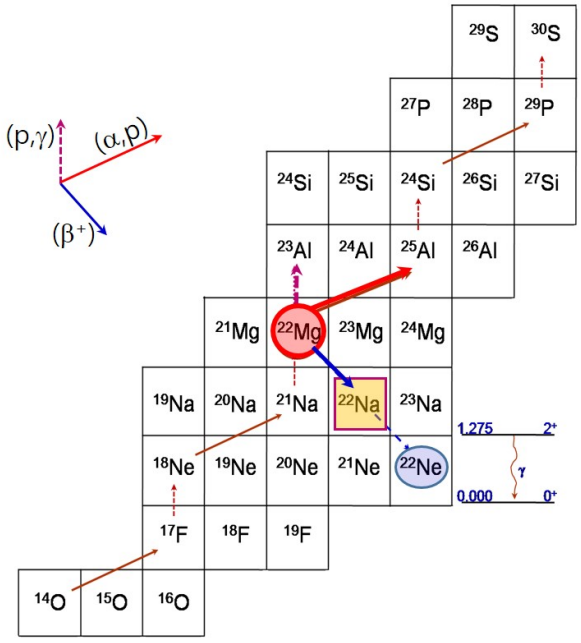

Fig. 4. The competition of the ^{22}Mg$(\alpha,p)^{25}$Al, ^{22}Mg$(p,\gamma)^{23}$Al reactions and β^+-decay at the waiting point ^{22}Mg in the nucleosynthesis impacts the 1.275-MeV gamma-ray observation and the ^{22}Na abundance.

In order to determine the astrophysical rates of the stellar reactions precisely, direct measurements are necessary. However, the direct method faces a significant challenge due to the low radioactive-isotope beam intensity and small cross section at the astrophysical energy. Hence, alternative methods of narrowing the uncertainty of the reaction rates are recommended. One indirect method is the evaluation of the rates by using the resonance states of the compound nucleus. In this method, the alpha and proton widths become significant in the calculation. The reaction rates are calculated based on the width as [4]

$$N_A\langle\sigma\nu\rangle = 1.54\times10^{11}(\mu T_9)^{-3/2}\sum_i(\omega\gamma)_i\exp\left(\frac{-11.605E_i}{T_9}\right)\left[\mathrm{cm^3\,s^{-1}\,mol^{-1}}\right], \tag{15}$$

where the resonant strengths $(\omega\gamma)_i$ (in MeV) of states i at resonant energies of E_i (in MeV) in center-of-mass system are calculated by

$$\omega\gamma = \frac{2J+1}{(2J_1+1)(2J_2+1)}\frac{\Gamma_1\Gamma_2}{\Gamma_{\mathrm{tot}}}\ [\mathrm{MeV}]\,. \tag{16}$$

In the equations above, J, J_1, and J_2 are the spins of the compound nucleus, the projectile and the target, respectively; Γ_1, Γ_2 are the alpha and proton widths, which are calculated by using Eq. (14), and $\Gamma_{\mathrm{tot}} = \Gamma_1 + \Gamma_2$ denotes the total width.

Since the NCPF computer code emerges as a useful tool to calculate the penetration factor, it is applied to determine the α-width of the ^{22}Mg$(\alpha,p)^{25}$Al reaction, which has been neither calculated nor measured recently. Subsequently, the astrophysical rates of the reaction are determined. According to the conservation rule [39], the angular momenta are assumed to be $l = 0$–4. The resonances of the compound nucleus, ^{26}Si, are proposed to be distributed at the excited states obtained by Matic *et al.* [40]. It should be noted that the excitation energies of the ^{26}Si nucleus were deduced from the transfer reaction ^{28}Si$(p,t)^{26}$Si. There were no proton- or α-width and spin-parity of the ^{26}Si states observed in the experiment. To calculate the widths, the term of C^2S containing the Clebsch–Gordan and the spectroscopic factors are assumed to be 0.01. Once the ^{22}Mg$(\alpha,p)^{25}$Al reaction proceeds, the α-width is much smaller than the proton width, $\Gamma_\alpha \ll \Gamma_p$. Hence, the total width is approximately equal to the proton width, $\Gamma_{\mathrm{tot}} \approx \Gamma_p$. Finally, the α-widths and resonant strengths corresponding to the assumed resonant energies of the compound nucleus, ^{26}Si, in the ^{22}Mg$(\alpha,p)^{25}$Al reaction are estimated, as listed in Table III.

TABLE III

The estimated α-widths and resonant strengths in the ^{22}Mg$(\alpha,p)^{25}$Al reaction.

No.	E_x [MeV]	$E_{\rm cm}$ [MeV]	J^π	Γ_α [MeV]	$\omega\gamma$ [MeV]
1	9.316	0.146	4^{+*}	7.93×10^{-42}	7.14×10^{-41}
2	9.373	0.203	0^+	1.20×10^{-31}	1.20×10^{-31}
3	9.433	0.263	1^-	7.27×10^{-27}	2.18×10^{-26}
4	9.606	0.436	2^{+*}	2.95×10^{-19}	1.48×10^{-18}
5	9.725	0.555	3^-	7.83×10^{-18}	5.48×10^{-17}
6	9.802	0.632	4^+	2.87×10^{-17}	2.58×10^{-16}
7	9.912	0.742	0^{+*}	7.62×10^{-12}	7.62×10^{-12}
8	10.070	0.900	1^-	3.96×10^{-10}	1.19×10^{-09}
9	10.297	1.127	2^+	1.26×10^{-08}	6.30×10^{-08}
10	10.405	1.235	3^-	1.31×10^{-08}	9.16×10^{-08}
11	10.688	1.518	4^+	6.40×10^{-08}	5.76×10^{-07}
12	10.827	1.657	0^+	5.72×10^{-05}	5.72×10^{-05}

*Spin-parities were assigned by Matic *et al.* [40]. The others are randomly chosen.

Once the resonant strengths are determined, the astrophysical rates of the ^{22}Mg$(\alpha,p)^{25}$Al reaction are calculated based on Eq. (15) with temperatures in the range of $T_9 = 0.1$–10. The evaluated rates are shown in Table IV. The contributions of the ^{22}Mg$(\alpha,p)^{25}$Al reaction rates from twelve resonant states of ^{26}Si are separately shown in Fig. 5. At temperatures $T_9 > 2.0$ GK, the higher excited energies give greater astrophysical reaction rates. The dominant contribution of the states depends on the temperature ranges. The 1.657-MeV (0^+) state yields the highest contribution in the range of $T_9 > 0.9$ GK, the 0.900-MeV (1^-) state is dominant at temperatures of 0.35–0.7 GK, the 0.742-MeV (0^+) state generates the highest rates in the range of $T_9 = 0.25$–0.35 GK, and the 0.436-MeV state is dominant in the range of $T_9 < 0.25$ GK.

As can be seen in Fig. 6, the rates calculated based on the Hauser–Feshbach model by using NON-SMOKER and TALYS codes at stellar temperatures of $T_9 < 1.5$ GK are about 2–4 times lower than the calculated values in this work, which is based on the observed excited states of ^{26}Si, whereas this manner inversely changes into 1–3 orders under conditions of the temperatures $T_9 > 3.0$ GK. While the present calculation is compatible with the estimation of the statistical model, the results in the study of Matic *et al.* [40] are much lower than the others in the temperature range of $T_9 > 0.7$ GK. Those low rates may be mainly caused by the lack of the resonances in ^{26}Si, which also contribute the reaction rates, considered in Ref. [40].

TABLE IV

Calculated astrophysical rates (in $\mathrm{cm^3\,mol^{-1}\,s^{-1}}$) of the $^{22}\mathrm{Mg}(\alpha,p)^{25}\mathrm{Al}$ reaction compared to the results obtained by Matic *et al.* [40] and the calculations of the Hauser–Feshbach model using the NON-SMOKER and TALYS codes.

T_9	This work	NON-SMOKER	TALYS	Matic *et al.* [40]
0.1	1.08×10^{-27}	8.07×10^{-30}	0.00×10^{00}	5.57×10^{-31}
0.2	4.80×10^{-18}	1.66×10^{-19}	7.80×10^{-24}	2.90×10^{-20}
0.3	5.45×10^{-13}	1.05×10^{-14}	9.95×10^{-17}	3.05×10^{-15}
0.4	9.07×10^{-10}	1.08×10^{-11}	3.21×10^{-13}	2.46×10^{-12}
0.5	1.10×10^{-07}	1.50×10^{-09}	4.87×10^{-11}	1.28×10^{-10}
0.6	3.37×10^{-06}	6.48×10^{-08}	2.38×10^{-09}	1.70×10^{-09}
0.7	4.66×10^{-05}	1.30×10^{-06}	5.88×10^{-08}	1.04×10^{-08}
0.8	3.96×10^{-04}	1.54×10^{-05}	8.09×10^{-07}	3.93×10^{-08}
0.9	2.47×10^{-03}	1.23×10^{-04}	7.21×10^{-06}	1.08×10^{-07}
1.0	1.21×10^{-02}	7.35×10^{-04}	4.70×10^{-05}	2.40×10^{-07}
1.5	2.39×10^{00}	3.64×10^{-01}	3.29×10^{-02}	2.28×10^{-06}
2.0	3.56×10^{01}	1.61×10^{01}	1.88×10^{00}	6.17×10^{-06}
3.0	4.63×10^{02}	1.48×10^{03}	2.44×10^{02}	1.40×10^{-05}
4.0	1.48×10^{03}	2.16×10^{04}	4.22×10^{03}	1.86×10^{-05}
5.0	2.76×10^{03}	1.32×10^{05}	2.74×10^{04}	2.05×10^{-05}
6.0	3.98×10^{03}	4.90×10^{05}	1.03×10^{05}	2.07×10^{-05}
7.0	4.99×10^{03}	1.32×10^{06}	2.72×10^{05}	2.02×10^{-05}
8.0	5.75×10^{03}	2.82×10^{06}	5.73×10^{05}	1.92×10^{-05}
9.0	6.29×10^{03}	5.08×10^{06}	1.03×10^{06}	1.82×10^{-05}
10.0	6.65×10^{03}	7.93×10^{06}	1.63×10^{06}	1.71×10^{-05}

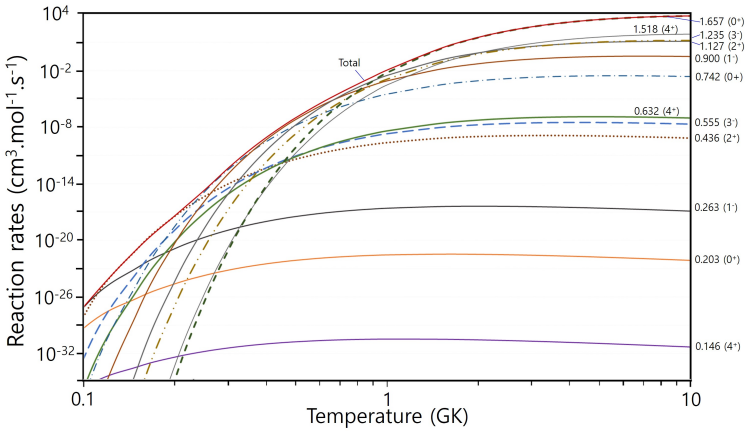

Fig. 5. The astrophysical rates (in $\mathrm{cm^3\,mol^{-1}\,s^{-1}}$) of the $^{22}\mathrm{Mg}(\alpha,p)^{25}\mathrm{Al}$ reaction as a function of stellar temperature T_9 (in GK) contributed by individual states presented together with the total rates.

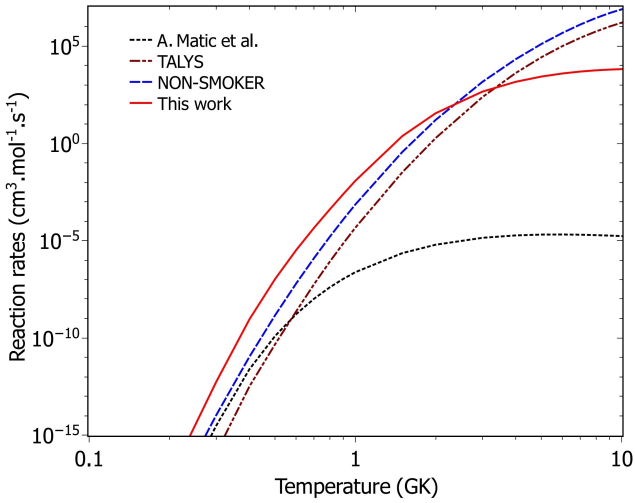

Fig. 6. The astrophysical rates of the ^{22}Mg$(\alpha,p)^{25}$Al reaction.

By comparing the astrophysical rates of the ^{22}Mg$(\alpha,p)^{25}$Al reaction calculated in the present work with the ^{22}Mg$(p,\gamma)^{23}$Al reaction rates, which were based on measurements of proton scattering of ^{22}Mg$+p$ by He [41], one can see that the ^{22}Mg$(\alpha,p)^{25}$Al rates are about 6.0 times higher than the other ones under the stellar temperature of $T_9 = 1.0$–3.0 GK, which are relevant for the conditions of type II-supernovae or X-ray bursts. However, the (p,γ) reaction rates are about 6.0 and 2.0 times higher than the (α,p) ones in the temperature ranges of $T_9 = 0.1$–0.5 GK and $T_9 = 0.5$–1.0 GK, respectively. In other words, under conditions of novae with stellar temperatures in the range of 0.1–1.0 GK, the (p,γ) reaction is dominant; subsequently, the competition at the waiting point ^{22}Mg mainly occurs between this reaction and the β^+-decay. The (α,p) reaction becomes stronger in the supernovae or X-ray bursts; hence, the competition between the (α,p) reaction and the decay becomes more significant at the waiting point ^{22}Mg.

3.3. NCPF for estimation of the α-decay half-life of heavy nuclei

After extensive testing of the NCPF code on astrophysical problems in the low-energy regime, we proceed to reproduce the half-lives of a series of even–even α-decay nuclei of which daughters have a spherical shape in the atomic number range of $Z = 52$–118, by using the expression in terms of the penetrability as [6]

$$T_{1/2} = \frac{\ln 2}{\xi P(Q)}\,, \tag{17}$$

where $P(Q)$ and ξ are, respectively, the penetration factor with Q-value of the α-decay and the deformation-independent parameter of nuclei, which can be determined by

$$\xi = \left(6.1814 + 0.2988A^{-1/6}\right) \times 10^{19} \times \exp\left(-13.116\beta\right)\ \mathrm{s}^{-1}. \qquad (18)$$

Here, A denotes the mass number of the parent nuclei and β is the deformed parameter of daughter nuclei, both of which are obtained from the database of Möller *et al.* (1995) [42]. It should be noted that the Q-values are almost out of the energy range for the AS approximation.

To validate the code and evaluate the semi-empirical formulae proposed by Viola and Seaborg [43] and by Poenaru and Ghergescu [44], we calculated the α-decay half-lives of nuclei with atomic numbers in the range of $Z = 52$–118 by using Eq. (17) and compared the results with the predictions of the formulae, the estimation by Li *et al.* [6], and experimental data [45, 46]. The penetration factor was calculated by the NCPF code, with the angular momenta carried by the α-particle of the α-core system at ground states assumed to be zero, $l = 0$. Despite using the same model of Eq. (17) with different methods to deduce the penetration factors, the half-lives determined based on the penetration factor calculated by the NCPF code are quite similar to those obtained by Li *et al.* [6], as can be seen in Table V. This good agreement indicates that the numerical calculation of the penetration factor in the present study is consistent with previous work. Moreover, the code

TABLE V

The decimal logarithmic half-lives (in seconds) of the α-decay nuclei with $Z = 52$–92 estimated by using different models were compared to the experimental data taken from Ref. [45].

ID	A	Q_α [MeV]	This work	Ref. [43]	Ref. [44]	Ref. [6]	Exp. [45]
$_{52}$Te	106	4.30	−4.32	−6.86	−4.42	− 3.83	−4.22
$_{60}$Nd	144	1.91	22.57	19.94	21.21	23.17	22.86
$_{64}$Gd	148	3.27	8.94	7.24	8.36	9.46	9.36
	150	2.81	13.52	11.53	12.59	13.91	13.75
$_{72}$Hf	156	6.03	−1.57	−3.21	−1.95	−1.66	−1.60
	158	5.40	0.58	−0.67	0.49	0.89	0.81
$_{84}$Po	205	5.33	6.31	6.97	6.19	6.72	7.18
	206	5.33	5.28	5.89	6.16	6.64	7.15
$_{86}$Rn	204	6.55	2.21	1.22	1.73	1.94	2.00
	206	6.38	1.84	1.89	2.33	2.56	2.74
$_{90}$Th	218	9.85	−6.86	−7.17	−6.59	−6.65	−6.96
	220	8.95	−5.12	−4.98	−4.49	−4.51	−5.01
$_{92}$U	222	9.43	−5.47	−5.51	−4.93	−5.20	−6.00

can be applied reliably to deduce the penetrability associated with the high-energy range ($E > E_{cr}$), out of the AS approximation which is available for the low-energy range ($E < E_{cr}$), for α-decay half-life estimations.

The estimated half-lives of transfermium and super-heavy nuclei with $Z = 94$–118 compared with the experimental data taken from Refs. [45, 46] are presented in Table VI. It is found that the half-lives calculated by the models depend on the odd–even numbers of protons and neutrons. In particular, all the models reproduce well the experimental data for the even–even nuclei, but not for the other cases (even–odd, odd–even, and odd–odd nuclei). In the case of even–odd nuclei, the half-lives estimated by Eq. (17) in this work and the Poenaru formula are closer to the experimental data than those obtained by the Viola and Seaborg relation and *vice versa* for the odd–even nuclei. Moreover, we found a large discrepancy between the calculations and measured data, highlighting a need for improvements in the theoretical models to improve predictions of the half-lives of the odd–odd isotopes.

4. Conclusion

In the present work, we successfully developed the NCPF computer code for numerically calculating the penetration factor for a wide range of energy cases. The NCPF is mainly based on Steed's method combined with a correction for the low-energy regime using the Abramowitz and Stegun approximation to evaluate the Coulomb functions. The code was validated by reproducing the penetration factor for astrophysical applications and estimation of the α-decay half-life of actinides. The validation results indicate that the NCPF code can be used reliably in penetrability calculations. We used the developed code to estimate the $^{22}\mathrm{Mg}(\alpha, p)^{25}\mathrm{Al}$ reaction rate, which is one of the most mysterious astrophysical problems. It was found that the $^{22}\mathrm{Mg}(\alpha, p)^{25}\mathrm{Al}$ reaction is dominant over proton capture of the $^{22}\mathrm{Mg}$ in novae, and *vice versa* in supernovae or X-ray bursts. On the other hand, the evaluation indicates that the α-decay half-life predictions have large uncertainty in odd–odd isotopes compared with experimental data. This highlights the need for more development of α-decay theories.

TABLE VI

The decimal logarithmic half-lives (in seconds) of the α-decay nuclei with estimated different models were compared to the experimental data taken from Duarte *et al.* [45] and Oganessian *et al.* [46].

ID	A	Q_α[MeV]	This work	Ref. [43]	Ref. [44]	Exp. [45]	ID	A	Q_α[MeV]	This work	Ref. [43]	Ref. [44]	Exp. [46]
$_{94}$Pu	228	7.95	−0.91	−0.54	0.10	−0.70	$_{106}$Sg	269	8.70	1.01	2.55	1.77	2.08
	233	6.41	7.43	6.48	5.60	6.00		271	8.67	1.01	2.65	1.83	1.98
	234	6.31	5.66	5.87	6.02	5.72	$_{107}$Bh	270	9.06	0.94	1.81	1.05	1.79
	235	5.95	9.75	8.69	7.71	7.75		271	9.42	−0.14	0.38	−0.02	0.18
	236	5.87	7.78	8.04	8.09	8.11		272	9.20	0.48	1.38	0.59	1.04
	238	5.59	9.33	9.54	9.53	9.59		274	8.94	1.10	2.18	1.34	1.64
	239	5.24	13.95	12.66	11.51	12.00	$_{108}$Hs	273	9.73	−0.69	0.12	−0.53	−0.70
	240	5.26	11.67	11.47	11.37	11.45		275	9.45	−0.07	0.92	0.21	−0.70
	244	4.67	15.63	15.42	15.15	15.51	$_{109}$Mt	274	10.20	−1.60	−0.79	−1.42	−0.36
$_{95}$Am	232	7.28	4.18	3.34	2.57	3.59		275	10.50	−2.43	−1.91	−2.19	−1.70
	237	6.19	8.96	7.68	7.02	7.18		276	10.05	−1.39	−0.39	−1.06	−0.35
$_{96}$Cm	240	6.40	6.49	6.37	6.49	6.52		278	9.58	−0.41	0.93	0.18	0.65
	244	5.90	8.99	8.84	8.83	8.88	$_{111}$Rg	278	10.85	−2.97	−1.83	−2.36	−2.38
	246	5.47	11.38	11.24	11.12	11.26		279	10.53	−2.29	−1.37	−1.60	−1.05
	248	5.16	13.30	13.15	12.95	13.15		280	10.15	−1.54	−0.02	−0.65	0.66
$_{98}$Cf	240	7.73	1.94	1.78	2.14	1.81		282	9.16	1.11	2.89	2.13	2.00
	244	7.33	3.41	3.27	3.51	3.18	$_{112}$Cn	285	9.32	0.79	2.68	1.98	1.45
	246	6.86	5.29	5.19	5.34	5.20	$_{113}$Nh	282	10.78	0.67	−1.05	−1.55	−1.14
	250	6.13	8.65	8.60	8.58	8.69		283	10.38	−1.85	−0.35	−0.56	−1.12
	254	5.93	9.57	9.65	9.53	9.30		284	10.20	−0.58	0.48	−0.10	−0.04
$_{99}$Es	253	6.74	7.88	6.93	6.20	6.30		285	10.01	−0.08	0.67	0.39	0.62

TABLE VI (continued)

ID	A	Q_α[MeV]	This work	Ref. [43]	Ref. [44]	Exp. [45]	ID	A	Q_α[MeV]	This work	Ref. [43]	Ref. [44]	Exp. [46]
$_{100}$Fm	245	8.44	0.80	1.20	0.56	0.62		286	9.79	0.53	1.64	0.98	0.98
	248	8.00	1.71	1.61	1.93	1.65	$_{114}$Fl	285	11.17	−2.01	−1.77	−2.18	−0.89
	252	7.15	4.83	4.83	4.98	4.15		286	10.35	−1.15	−0.73	−0.16	−0.92
	256	7.03	5.21	5.33	5.39	5.15		287	10.17	−0.55	0.83	0.30	−0.32
$_{101}$Md	247	8.92	0.62	−0.22	−0.51	0.46		288	10.07	−0.92	0.05	0.55	−0.18
$_{102}$No	250	8.96	−0.63	−0.76	−0.29	−0.30		289	9.98	0.45	1.37	0.78	0.28
	252	8.55	0.37	0.52	0.91	0.62	$_{115}$Mc	287	10.76	−1.75	−0.74	−0.86	−1.43
	254	8.23	1.58	1.58	1.90	1.86		288	10.70	−1.62	−0.24	−0.73	−0.79
	258	8.15	2.35	1.85	2.09	2.08		289	10.49	−1.10	−0.02	−0.21	−0.48
	259	7.85	4.35	3.97	3.09	> 5.28		290	10.41	−0.90	0.53	−0.02	−0.19
$_{103}$Lr	252	9.16	0.54	0.10	−0.51	−0.40	$_{116}$Lv	290	11.00	−2.20	−1.82	−1.15	−2.08
$_{104}$Rf	253	9.55	−1.76	−0.71	−1.20	0.56		291	10.89	−1.75	−0.47	−0.90	−1.72
	254	9.38	−0.18	−1.30	−0.76	−0.77		292	10.78	−2.48	−1.26	−0.64	−1.89
	258	9.33	−0.11	−1.15	−0.70	−0.96		293	10.71	−2.06	−0.01	−0.48	−1.24
	260	8.90	0.04	0.13	0.50	0.00	$_{117}$Ts	293	11.32	−2.27	−1.55	−1.62	−1.66
$_{105}$Db	255	9.72	−1.91	−1.14	−1.31	0.30		294	11.18	−2.27	−0.86	−1.30	−1.29
	261	9.23	−0.73	0.25	−0.08	< 0.56	$_{118}$Og	294	11.82	−2.53	−3.22	−2.43	−2.16
$_{106}$Sg	260	9.93	−2.12	−2.15	−1.58	−2.07							
$_{108}$Hs	264	10.59	−3.16	−3.22	−2.56	−4.00							
	265	10.44	−2.24	−1.78	−2.21	−2.74							
$_{110}$Ds	269	11.68	−4.52	−4.10	−4.40	−3.77							
	277	10.72	−2.74	−1.86	−2.39	−2.22							
$_{111}$Rg	272	11.23	−3.39	−2.74	−3.13	>-2.82							

We are grateful to Prof. Alain Coc for explaining the numerical data in his published paper and Dr. Shun Ohgoda for fruitful discussion of the programming. This work was supported by the National Research Foundation of Korea (NRF) grants funded by the Korean government (MEST) (Nos. NRF-2017R1D1A1B03030019, NRF-2019R1F1A1058370), and the Vietnam Government under the Program of Development in Physics toward 2020 (grant No. DTDLCN.02/19). This work is also funded by the Vietnam National Foundation for Science and Technology Development (NAFOSTED) under grant No. 103.04-2018.303. T.V. Nhan Hao (tvnhao@hueuni.edu.vn) also thanks the Hue University for financial support through grant No. 43/HD-DHH for the Nuclear Physics Research Group (NP@HU).

REFERENCES

[1] G. Gamow, «Zur quantentheorie des atomkernes», *Z. Phys.* **51**, 204 (1928).

[2] E.U. Condon, R.W. Gurney, «Wave mechanics and radioactive disintegration», *Nature* **122**, 439 (1928).

[3] R.W. Gurney, E.U. Condon, «Quantum mechanics and radioactive disintegration», *Phys. Rev.* **33**, 127 (1929).

[4] C.E. Rolfs, W.S. Rodney, «Cauldrons in the cosmos: Nuclear astrophysics», *University of Chicago Press*, Chicago 1988.

[5] V.Y. Denisov, H. Ikezoe, «α-nucleus potential for α-decay and sub-barrier fusion», *Phys. Rev. C* **72**, 064613 (2005).

[6] L.L. Li, S.G. Zhou, E.G. Zhao, W. Scheid, «A new barrier penetration formula and its application to alpha-decay half-lives», *Int. J. Mod. Phys. E* **19**, 359 (2010).

[7] B. Buck, J.C. Johnston, A.C. Merchant, S.M. Perez, «Cluster model of α decay and ^{212}Po», *Phys. Rev. C* **53**, 2841 (1996).

[8] D.L. Hill, J.A. Wheeler, «Nuclear constitution and the interpretation of fission phenomena», *Phys. Rev.* **89**, 1102 (1953).

[9] J. Humblet, W.A. Fowler, B.A. Zimmerman, «Approximate penetration factors for nuclear reactions of astrophysical interest», *Astron. Astrophys.* **177**, 317 (1987).

[10] E.C. Kemble, «A contribution to the theory of the B.W.K. method», *Phys. Rev.* **48**, 549 (1935).

[11] C. Xu, Z. Ren, «Systematical calculation of α decay half-lives by density-dependent cluster model», *Nucl. Phys. A* **753**, 174 (2005).

[12] M. Abramowitz, I. Stegun, «Handbook of mathematical functions: with formulas, graphs, and mathematical tables», *Courier Corporation*, 1965.

[13] E.F. Brown, «Implications of a subthreshold resonance for stellar beryllium depletion», *Astrophys. J.* **495**, 905 (1998).

[14] M. Wiescher, Department of Physics, University of Notre Dame, private communication.

[15] C. Wheldon, Kinematics and Q-values: ckin.c, 2018, http://www.np.ph.bham.ac.uk/research_resources/programs/

[16] R. Smith *et al.*, «Evidence for a 3.8 MeV state in ^{9}Be», *Phys. Rev. C* **94**, 014320 (2016).

[17] I.J. Thompson, A.R. Barnett, «COULCC: A continued-fraction algorithm for Coulomb functions of complex order with complex arguments», *Comput. Phys. Commun.* **36**, 363 (1985).

[18] A.R. Barnett, «The calculation of spherical Bessel and Coulomb functions», in: E. Bartschat (Ed.) «Computational Atomic Physics», *Springer*, Berlin, Heidelberg 1996, pp. 181–202.

[19] J.W. Steed, Ph.D. dissertation, University of Manchester, 1967.

[20] A.R. Curtis (Ed.), «Royal Society Mathematical Tables, Volume 11: Coulomb wave functions», *Cambridge University Press*, London 1964.

[21] A.R. Barnett, D.H. Feng, J.W. Steed, L.J.B. Goldfarb, «Coulomb wave functions for all real η and ϱ», *Comput. Phys. Commun.* **8**, 377 (1974).

[22] C. Bardinr *et al.*, «Coulomb functions in entire (η, ϱ)-plane», *Comput. Phys. Commun.* **3**, 73 (1972).

[23] K.L. Bell, N.S. Scott, «Coulomb functions (Negative energies)», *Comput. Phys. Commun.* **20**, 447 (1980).

[24] M.J. Seaton, «Coulomb functions analytic in the energy», *Comput. Phys. Commun.* **25**, 87 (1982).

[25] L.Y. Peng, Q. Gong, «An accurate Fortran code for computing hydrogenic continuum wave functions at a wide range of parameters», *Comput. Phys. Commun.* **181**, 2098 (2010).

[26] A.R. Barnett, «Continued-fraction evaluation of Coulomb functions $F_\lambda(\eta, x), G_\lambda(\eta, x)$ and their derivatives», *J. Comput. Phys.* **46**, 171 (1982).

[27] C. Schwartz, «Numerical calculation of Bessel functions», *Int. J. Mod. Phys. C* **23**, 1250084 (2012).

[28] C. Lanczos, «A precision approximation of the Gamma function», *J. SIAM Numer. Anal.* **1**, 86 (1964).

[29] E. Kuulkers *et al.*, «X-ray bursts at extreme mass accretion rates from GX 17+2», *Astron. Astrophys.* **382**, 947 (2002).

[30] W. Penninx *et al.*, «EXOSAT observations of the X-ray burst source 4U 1608-52», *Astron. Astrophys.* **208**, 146 (1989).

[31] M. Sztajno *et al.*, «Unusual X-ray burst profiles from 4U/MXB 1636-53», *Astrophys. J.* **299**, 487 (1985).

[32] A. Coc, F. Hammache, J. Kiener, «Recent results in nuclear astrophysics», *Eur. Phys. J. A* **51**, 34 (2015).

[33] R.J. deBoer *et al.*, «The ^{12}C$(\alpha,\gamma)^{16}$O reaction and its implications for stellar helium burning», *Rev. Mod. Phys.* **89**, 035007 (2017).

[34] S. Almaraz-Calderon *et al.*, «Level structure of ^{30}S and its importance in the ^{26}Si$(\alpha,p)^{29}$P and ^{29}P$(p,\gamma)^{30}$S reaction rates», *Phys. Rev. C* **86**, 065805 (2012).

[35] A.F. Iyudin *et al.*, «Global galactic distribution of the 1.275 MeV γ-ray line emission», *Astron. Astrophys.* **443**, 477 (2005).

[36] J.C. Higdon, W.A. Fowler, «Gamma-ray constraints on Na-22 yields in nova explosions», *Astrophys. J.* **317**, 710 (1987).

[37] M. Arnould *et al.*, «Thermonuclear origin of Ne-*E*», *Astron. Astrophys.* **64**, 195 (1978).

[38] W. Hillebrandt, F.K. Thielemann, «Nucleosynthesis in novae — A source of Ne-E and Al-26», *Astrophys. J.* **255**, 617 (1982).

[39] A. Das, T. Ferbel, «Introduction to nuclear and particle physics», *World Scientific*, 2003.

[40] A. Matic *et al.*, «High-precision ^{28}Si$(p,t)^{26}$Si reaction to determine ^{22}Mg$(\alpha,p)^{25}$Al reaction rates», *Phys. Rev. C* **84**, 025801 (2011).

[41] J.J. He *et al.*, «Investigation of structure in ^{23}Al via resonant proton scattering of ^{22}Mg + p and the ^{22}Mg$(p,\gamma)^{23}$Al astrophysical reaction rate», *Phys. Rev. C* **76**, 055802 (2007).

[42] P. Möller *et al.*, «Axial and reflection asymmetry of the nuclear ground state», *Atom. Data Nucl. Data Tables,* **94**, 758 (2008).

[43] V.E. Viola. Jr., G.T. Seaborg, «Nuclear systematics of the heavy elements — II lifetimes for alpha, beta and spontaneous fission decay», *J. Inorg. Nucl. Chem.* **28**, 741 (1966).

[44] D N. Poenaru, R.A. Gherghescu, «α decay and cluster radioactivity of nuclei of interest to the synthesis of $Z = 119$, 120 isotopes», *Phys. Rev. C* **97**, 044621 (2018).

[45] S.B. Duarte *et al.*, «Half-lives for proton emission, alpha decay, cluster radioactivity, and cold fission processes calculated in a unified theoretical framework», *Atom. Data Nucl. Data Tables* **80**, 235 (2002).

[46] Y.T. Oganessian, V.K. Utyonkov, «Superheavy nuclei from ^{48}Ca-induced reactions», *Nucl. Phys. A* **944**, 62 (2015).